7-9-2003

Uncertainties in Precipitation and Their Impacts on Runoff Estimates

Balazs M. Fekete
University of New Hampshire, Durham

Charles J. Vörösmarty
CUNY City College

John O. Roads
University of California, San Diego

Cort J. Willmott
University of Deleware

Uncertainties in Precipitation and Their Impacts on Runoff Estimates

BALÁZS M. FEKETE AND CHARLES J. VÖRÖSMARTY

Institute for the Study of Earth, Oceans, and Space, University of New Hampshire, Durham, New Hampshire

JOHN O. ROADS

Scripps Institution of Oceanography, University of California, San Diego, La Jolla, California

CORT J. WILLMOTT

Department of Geography, University of Delaware, Newark, Delaware

(Manuscript received 17 March 2003, in final form 9 July 2003)

ABSTRACT

Water balance calculations are becoming increasingly important for earth-system studies. Precipitation is one of the most critical input variables for such calculations because it is the immediate source of water for the land surface hydrological budget. Numerous precipitation datasets have been developed in the last two decades, but these datasets often show marked differences in their spatial and temporal distribution of this key hydrological variable. This paper compares six monthly precipitation datasets—Climate Research Unit of University of East Anglia (CRU), Willmott–Matsuura (WM), Global Precipitation Climate Center (GPCC), Global Precipitation Climatology Project (GPCP), Tropical Rainfall Measuring Mission (TRMM), and NCEP–Department of Energy (DOE) Atmospheric Model Intercomparison Project (AMIP-II) Reanalysis (NCEP-2)—to assess the uncertainties in these datasets and their impact on the terrestrial water balance. The six datasets tested in the present paper were climatologically averaged and compared by calculating various statistics of the differences. The climatologically averaged monthly precipitation estimates were applied as inputs to a water balance model to estimate runoff and the uncertainties in runoff arising directly from the precipitation estimates. The results of this study highlight the need for accurate precipitation inputs for water balance calculations. These results also demonstrate the need to improve precipitation estimates in arid and semiarid regions, where slight changes in precipitation can result in dramatic changes in the runoff response due to the nonlinearity of the runoff-generation processes.

1. Introduction

Water balance calculations are important in both climate research and biosphere studies since they provide essential information on the amount of water circulating in the hydrological cycle and the amount of renewable water available for ecosystems and human society. The water budget over a unit land surface area is normally expressed as $R = P - E - dS/dt$, where P is precipitation [length/time (L/T)], E is evapotranspiration (L/T), dS/dt is change in surface water storage (L/T) and R is excess water (runoff) (L/T) (Thornthwaite 1948; Thornthwaite and Mather 1955; Willmott et al. 1985a; Vörösmarty et al. 1989). In this equation, precipitation is the only climate variable measured directly on a regular basis.

Corresponding author address: Dr. Balázs M. Fekete, Water Systems Analysis Group, Institute for the Study of Earth, Oceans, and Space, University of New Hampshire, Morse Hall, Rm. 211, 39 College Road, Durham, NH 03824-3525.
E-mail: balazs.fekete@unh.edu

Precipitation is one of the most important climate variables for determining accurate water balance calculations since it is the predominant and ultimate source of water for the land surface water budget. In the last 2 decades, numerous global precipitation datasets have been developed using different input sources such as ground observations, satellite estimates, and climate model simulations. These datasets typically agree in the major temporal trends and spatial distribution of the precipitation (i.e., over latitudinal bands and seasonal cycles), but they often show marked differences regionally (Costa and Foley 1998; Adler et al. 2001). The reliability of the station-based data products was found to be closely related to the rain gauge density (Oki et al. 1999). The present paper compares a series of precipitation datasets to assess the degree of uncertainty among them and to estimate the impact of the uncertainty on remaining components of the terrestrial water cycle.

We compare six global, monthly, gridded precipitation climatological datasets [Climate Research Unit (CRU) (New et al. 1999, 2000; CRU 2000), Willmott–

Matsuura (WM; Willmott and Matsuura 2001), Global Precipitation Climate Center (GPCC; Rudolf et al. 1994; GPCC 2001), Global Precipitation Climatology Project (GPCP; Huffman et al. 1995; GPCP 1998), Tropical Rainfall Measuring Mission (TRMM; Huffman et al. 1997; Huffman 1997), and the National Centers for Environmental Prediction–Department of Energy (NCEP–DOE) Atmospheric Model Intercomparison Project (AMIP-II) Reanalysis (NCEP-2; Kanamitsu et al. 2002)] to understand the spatial and seasonal differences between the different datasets. The different precipitation data products along with other climate and land surface variables were applied in a global water balance model (WBM; Federer et al. 1996, 2003; Vörösmarty et al. 1998, 1996). All WBM calculations used the same climate input data from CRU (except for precipitation) and the same land surface characterization (i.e., same land cover and soil types).

2. Method

a. Global gridded precipitation datasets

The CRU at the University of East Anglia developed both mean monthly climatologies and time series (1901–95) of various climate variables including precipitation (New et al. 1999, 2000). They collected station data from various (formal and informal) sources and applied thin-spline interpolation (Hutchinson 1995; Wahba 1979). They adopted Willmott et al.'s (1995, 1996) approach by developing a climatology first from relaxed time series consistency and superimposed interannual anomalies based on stations with sufficiently long records (New et al. 1999). The CRU dataset was developed at several resolutions and we used their $0.5^\circ \times 0.5^\circ$ (latitude $\times$ longitude) resolution fields.

The WM global precipitation dataset (Willmott and Matsuura 2001) at $0.5^\circ \times 0.5^\circ$ resolution (latitude $\times$ longitude in geographical coordinates) was developed at the Department of Geography at the University of Delaware. This dataset grew out of the earlier Legates and Willmott precipitation dataset (Legates and Willmott 1990). The Legates and Willmott climatologies were among the first global datasets that broke the tradition of using stations only with temporally commensurate records. They argued that the spatial variation of climate fields at large scales are more significant than the interannual variation; therefore, the inclusion of all available stations to resolve the spatial heterogeneity is more important than to maintain rigorous time series consistency (Willmott et al. 1996). The original Legates and Willmott (1990) datasets were only available as long-term climatologies. The recently released Willmott–Matsuura dataset is based on the same philosophy as well as on climatologically aided interpolation. It also used an improved version of the Shepard interpolation algorithm (Shepard 1968; Willmott et al. 1985b) and a more robust neighbor-finding method. The maximum number of nearby stations considered in the interpolation was increased from 7 to 20, resulting in smaller cross-validation errors and ''visually more realistic'' precipitation fields (Willmott and Matsuura 2001). Furthermore, this new dataset is available as a time series covering the 1950–99 period.

The GPCC hosted at the German Weather Service (Deutscher Wetterdinst, Offenbach, Germany) is the official precipitation data center of the World Meteorological Organization (WMO). GPCC operationally collects and archives global precipitation data and develops derived data products (Rudolf et al. 1994). GPCC has data for ~48 000 land stations and near-real-time access to 6000–7000 Synoptic Ocean Prediction (SYNOP) and conveyable low-noise infrared radiometer for measurements of atmosphere and ground surface targets (CLIMAT) reports via the WMO's Global Telecommunication System (GTS). GPCC is developing verification data products (using their entire data archive) and monitoring products (based on the SYNOP and CLIMAT data). Unfortunately, the verification product is not available yet, therefore the monitoring product—which is available near real time (with 2-month time lag) from 1986 to present at $1^\circ \times 1^\circ$ resolution—was used in this intercomparison. GPCC also provides separate gauge correction data using the Legates and Willmott (1990) method to account for the well-known problem of gauge undercatch. This monitoring data product with the gauge correction provides the ground truthing for the Global Precipitation Climatology Project outputs.

The GPCP as part of the Global Energy and Water Cycle Experiment (GEWEX) of the World Climate Research Program, was established to develop monthly precipitation data products based on remotely sensed data from geostationary and polar-orbiting satellites plus ground observations. The currently available GPCP products (versions 1.c and 2.x) combine precipitation estimates from microwave [Special Sensor Microwave Imager (SSM/I)] and infrared sensors at $2.5^\circ \times 2.5^\circ$ resolution and GPCC ground-based precipitation estimates with gauge correction. The version 1.c and the version 2.x products are very similar, except that the version 2.x product incorporates TIROS Operational Vertical Sounder (TOVS) and outgoing longwave radiation (OLR) Precipitation Index (OPI) for time periods when SSM/I was not available (Susskind et al. 1997). The version 1.c product covers the time period of 1986 through present while the version 2.x product is available for 1979 to present.

The TRMM is a joint mission between the National Space Development Agency (NASDA) of Japan and the National Aeronautics and Space Administration (NASA) of the United States. The mission was designed to study tropical rainfall between 35°N and 35°S. The TRMM satellite carries five different instruments [the first space-borne Precipitation Radar (PR), TRMM Microwave Imager (TMI), Visible and Infrared Scanner (VIRS), Clouds and the Earth's Radiant Energy System

sensor (CERES), Lightning Imaging Sensor]. The TRMM community developed and distributes a large array of data products ranging from the raw remote sensing data to higher-level outputs including various precipitation estimates. In the present study, we used the 3B43 product, which was developed to provide the ''best estimate'' of precipitation based on TRMM and other data including GPCC precipitation estimates. This data product developed at $1^\circ \times 1^\circ$ resolution is continously updated and available in semi–real time with a few months lag. For this study, we used the 1998–2001 period that was available with complete annual cycle at the time of the presented analysis.

The NCEP-DOE AMIP-II Reanalysis (R-2) is a follow-up to the NCEP–National Center for Atmospheric Research (NCAR) reanalysis (Kistler et al. 2001; Kalnay et al. 1996). The original NCEP–NCAR reanalysis covers the 1950–2001 period while the new NCEP-2 product is available from 1979–present. This reanalysis product incorporates observational data (such as surface meteorological stations, ships, aircraft, rawinsonde, and satellite) with numerical weather forecast simulation. The developers of the NCEP–NCAR and the NCEP-2 reanalysis products mark clearly the degree to which a particular variable is simulated or observed. The precipitation is mostly simulated. The differences between the original NCEP–NCAR reanalysis and the new NCEP-2 products are discussed in Roads et al. (1999, 2002) and Roads (2003). The reanalysis product is available on a roughly $2.5^\circ \times 2.5^\circ$ resolution global grid and the output variables are archived as 6-hourly integrals.

b. Meteorological variables

The evapotranspiration term of the water balance equation is normally not measured directly over broad domains, therefore it has to be estimated considering the state of the atmosphere and the available water for evapotranspiration. The number of variables required for the calculation of the evapotranspiration varies by the sophistication of the applied methods. The simpler ones require air temperature and sometimes solar radiation, while the more complex ones additionally require vapor pressure, wind speed, and diurnal variation of air temperature (Federer et al. 1996).

The CRU dataset has all the variables needed for evaporation estimates. Some of the variables (air temperature, cloud coverage, and vapor pressure) are available as time series similar to the precipitation datasets for the 1901–95 time period. Others were developed as long-term mean only (wind speed). In the present study, we used the CRU datasets for each meteorological variable needed by the water balance model with the exception of precipitation.

c. Water balance model configuration

UNH's water balance model (Vörösmarty et al. 1998, 1989) configured with the Shuttleworth and Wallace (1985) potential evaporation (PET) function was used to test the different precipitation datasets. The Shuttleworth and Wallace PET method is one of the most data-extensive PET functions, which considers all elements (such as evaporation from soil and leaves as well as transpiration from the plant) by calculating resistance terms from the different evaporating surfaces. Nonetheless, the availability of vapor pressure, cloud coverage, and wind speed from the CRU dataset makes it possible to use such a complex PET calculation scheme at the global scale.

The land surface characterization was developed by Melillo et al. (1993), which was translated to seven major land surface categories (conifer forest, broad-leaf forest, savannah, grassland, tundra, desert, and open water). These major land-use categories were found to have distinct evaporation characteristics (Federer et al. 1996; Vörösmarty et al. 1998). Dominant soil texture was from United Nations Food and Agriculture Organization (FAO) soil maps (FAO/UNESCO 1986). The combination of the major land-use categories and the soil texture was used to determine rooting depth (Vörösmarty et al. 1998). Soil texture was also used to parameterize soil properties such as porosity, maximum capacity, and wilting point.

3. Comparison of precipitation datasets

a. Assessing the degree of inconsistency among precipitation datasets

The six precipitation datasets compared in the present study have inconsistencies in spatial resolution, temporal coverage, and methodology. As was discussed in section 2a, some of the datasets were only available at coarser resolutions (GPCC and TRMM at 1°, GPCP and NCEP-2 at ~2.5°). These datasets were interpolated to 30-min resolution using an inverse distance-weighted ''4-6-9 point'' interpolation (Fekete 2001).

The impact of differences in spatial resolution was tested on the Willmott–Matsuura dataset. First the 30′ resolution annual precipitation was aggregated to 1° and 2.5°, then the aggregated fields were interpolated to 30′ resolution. The regridded fields were compared to the original dataset. This comparison showed that the degradation and interpolation could cause substantial local differences but preserved sufficiently the large-scale patterns of the original precipitation field and introduced negligible bias (1.3 and 3.4 mm, respectively) (Table 1).

Besides the resolution differences, these datasets represent different observation periods. The CRU dataset represents 1901–95, GPCC and GPCP are available for 1986 to present, the NCEP-2 dataset used in the present study covers 1979–present, while Willmott–Matsuura

TABLE 1. Comparison of mean annual precipitation at different resolutions. The Willmott–Matsuura datasets at 0.5° resolution were aggregated to 1° and 2.5° and the aggregated coarser-resolution datasets were interpolated back to 0.5°. The table summarizes the comparison of the original gridded fields to the reinterpolated fields to assess the impact of comparing datasets from different resolutions. The first row contains the mean annual precipitation over the continental landmass depicted by the original Willmott–Matsuura dataset and regridded datasets. The three cross-matrices give mean absolute difference (MAD), root-mean-square error (rmse) and the bias.

	30 min	1°	2.5°
Mean	697.6	698.9	701.0
	Mean absolute difference (MAD)		
30 min	0.0	37.2	77.9
1°	37.2	0.0	53.6
2.5°	77.9	53.6	0.0
	Root-mean-square error (rmse)		
30 min	0.0	98.9	178.6
1°	98.9	0.0	114.2
2.5°	178.6	114.2	0.0
	Bias		
30 min	0.0	−1.3	−3.4
1°	1.3	0.0	−2.2
2.5°	3.4	2.2	0.0

was available for the 1950–99 period. Since five out of the six datasets were available between 1986 and 1995, this period was chosen as the common time frame for calculating monthly and annual climatologies (Fig. 1).

The TRMM dataset was available only for the 1998–2001 period. The effect of this inconsistency in comparing 1998–2001 TRMM climatology to the 1986–95 climatologies of the five other datasets was assessed by comparing the 1986–95 and 1998–2001 climatologies of GPCC and GPCP (the two datasets, which covered both the common 1986–95 and the TRMM 1998–2001 periods). Figure 2 shows the latitudinal profiles mean annual precipitation derived from the 1986–95 (P_{10yr}) and 1998–2001 (P_{3yr}) periods from the two datasets along with the frequency distribution of their absolute ($P_{3yr} - P_{10yr}$) and relative differences [$(P_{3yr} - P_{10yr})/(P_{3yr} + P_{10yr})$].

The remarkable similarity of the climatologies derived from different observation periods strongly supports Legates and Willmott's argument that at large scales the spatial variation of the precipitation is much more important than the interannual variation.

b. *Comparison of mean annual precipitation estimates from the different global monthly datasets*

Table 2 summarizes the mean annual precipitation differences between the five datasets, which were available for the 1986–95 period. The mean annual precipitation over global landmass varies between 653.8 mm yr^{-1} (GPCC) and 804.4 mm yr^{-1} (NCEP-2). The Willmott–Matsuura and the CRU datasets appear to be almost identical with 697.2 and 697.6 mm yr^{-1} annual mean precipitation. Despite their similarity with the 10-yr mean global annual precipitation, the mean absolute difference (MAD) between the two datasets (based on one-to-one grid comparison) is high (91.2 mm yr^{-1}, which is almost as high as the mean absolute deviation from the other datasets), suggesting that the two datasets have marked local differences.[1] The opposite is the case with GPCC and GPCP. These two datasets appear to be largely different in terms of mean annual precipitation over land yet the mean absolute deviation of the two datasets is relatively low (110.8 mm yr^{-1}, considering the high bias 70.8 mm yr^{-1}).

The NCEP-2 data product stands out from the other four datasets both in terms of the mean annual precipitation over land and the mean absolute deviation of NCEP-2 from any other datasets. The NCEP-2 dataset

[1] We calculate and report both the MAD and the rmse, although we interpret only the MAD. While rmse is reported commonly in the literature, it is a function of both the average error and the distribution of errors, rather than of average of error exclusively. We interpret MAD, since it is the natural, unambiguous measure of average error alone.

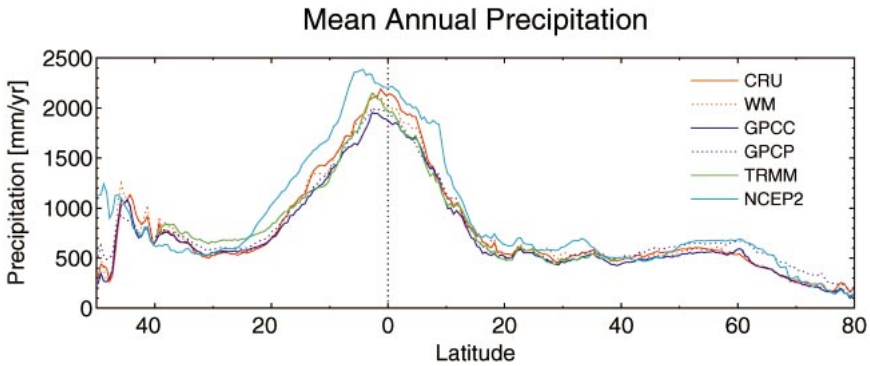

FIG. 1. Latitudinal profiles of the CRU, WM, GPCC, GPCP, NCEP-2, and TRMM mean annual precipitation datasets.

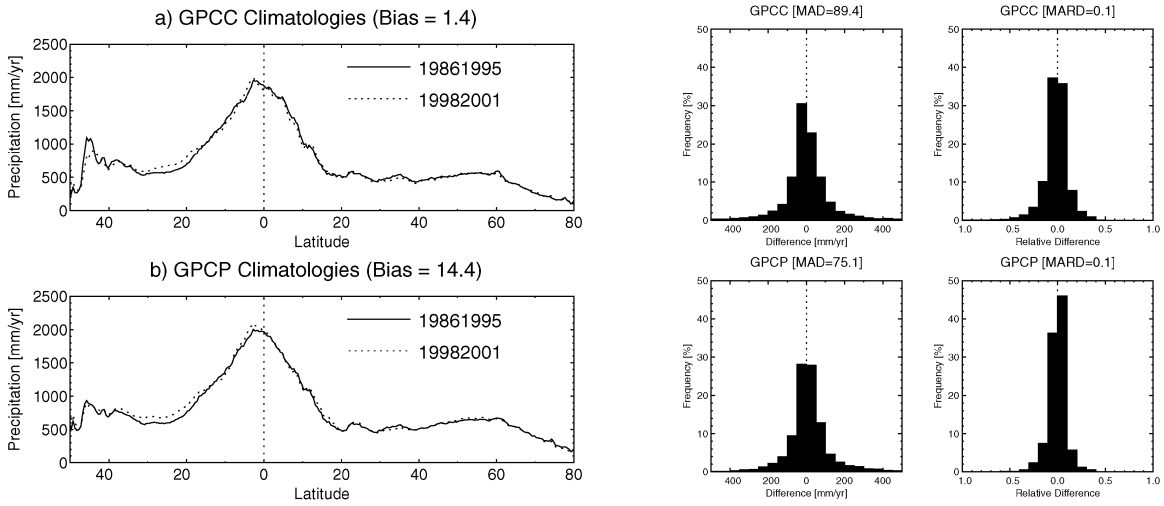

FIG. 2. Comparison of 1986–95 mean annual precipitation according to GPCC and GPCP to annual mean of the 1998–2001 period. The latitudinal profiles (a) GPCC and (b) GPCP show minor differences, which is also reflected in the low bias (1.4 and 14.4 mm yr^{-1} according to GPCC and GPCP, respectively) between the mean annual precipitation based on the different sampling periods. The frequency distribution of the absolute and relative deviations (presented next to the latitudinal profiles) show more significant differences [the mean absolute deviation (MAD) between the different climatologies of GPCC and GPCP are 89.4 and 75.4 mm yr^{-1}, respectively, while the relative deviation for both datasets is ~10%].

appears to be very different both regionally (mean absolute deviation well over 200 mm yr^{-1}) and in depicting the mean annual precipitation globally (~80 to 150 mm yr^{-1} bias) compared to the other datasets (Table 2).

Figure 1 shows the latitudinal profiles of the six precipitation climatologies. Although all of them depict the same precipitation patterns, the differences among them far exceed the differences that can be attributed to inconsistency in spatial resolution or temporal coverage. The latitudinal profiles reveal more details about the differences between the datasets. The NCEP-2 is the highest at almost all latitudes. GPCC and GPCP are very similar in the midlatitudes, but depart significantly at the higher latitudes. Apparently, the large difference in terms of the mean annual average over land is largely due to the differences between the two datasets across the higher latitudes. CRU and WM are very similar at all latitudes.

TABLE 2. Comparison of mean annual precipitation fields. The first row contains the mean annual precipitation over the continental landmass depicted by five precipitation datasets. The three cross-matrices give mean absolute difference (MAD), root-mean-square error (rmse) and the bias between the datasets.

	CRU	WM	GPCC	GPCP	NCEP2
Mean	697.2	697.6	653.8	724.8	804.4
			Mean absolute difference (MAD)		
CRU	0.0	91.2	102.4	138.7	246.3
WM	91.2	0.0	105.4	147.8	252.6
GPCC	102.4	105.4	0.0	110.8	243.1
GPCP	138.7	147.8	110.8	0.0	224.0
NCEP2	246.3	252.6	243.1	224.0	0.0
			Root-mean-square error (rmse)		
CRU	0.0	189.1	228.1	247.2	437.0
WM	189.1	0.0	236.6	261.5	446.0
GPCC	228.1	236.6	0.0	163.0	431.8
GPCP	247.2	261.5	163.0	0.0	394.3
NCEP2	437.0	446.0	431.8	394.3	0.0
			Bias		
CRU	0.0	−0.4	43.1	−27.6	−107.1
WM	0.4	0.0	43.5	−27.2	−106.7
GPCC	−43.1	−43.5	0.0	−70.8	−150.3
GPCP	27.6	27.2	70.8	0.0	−79.6
NCEP2	107.1	106.7	150.3	79.6	0.0

In lieu of all the possible one-to-one combinations, an ensemble dataset based on the four most similar datasets (CRU, WM, GPCC, GPCP) was developed as a reference against which the individual datasets could be compared. Figure 3 shows the frequency distribution of the differences between the ensemble mean annual precipitation versus the six tested datasets. The four datasets used for the reference ensemble datasets shows much similarity, while both the NCEP-2 and the TRMM data products have larger deviations from the ensemble datasets than the other four.

The difference between TRMM and the ensemble data is partly due to the difference in geographic extents and observation periods as discussed in sections 2a and 3a. When a similar comparison is performed among the six datasets for the TRMM domain only, the TRMM datasets appears to be more similar to the ensemble datasets but still stand out. This suggest that the TRMM product gives less weight to the ground-based observations than the ensemble datasets.

The high disparity between the NCEP-2 and the en-

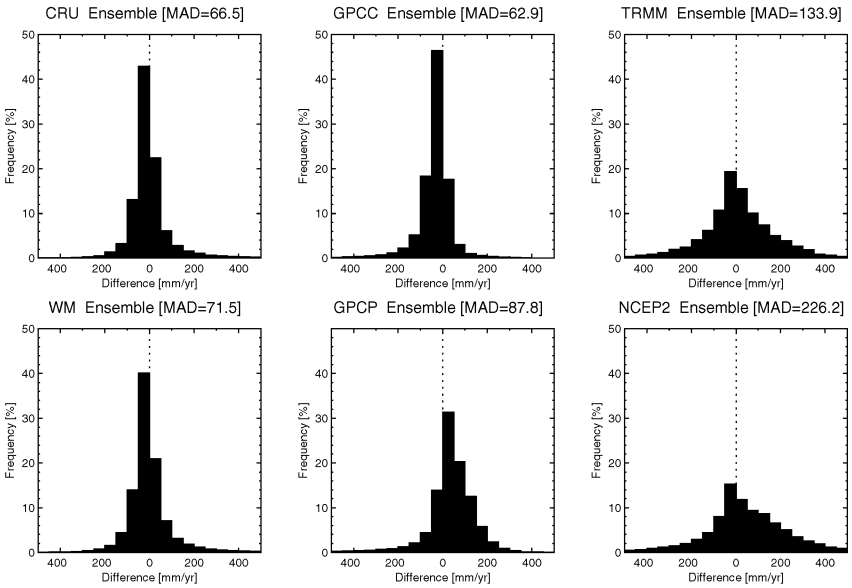

FIG. 3. Frequency distribution of the difference in mean annual precipitation from the tested data products and the reference ensemble dataset developed by averaging the most similar four data products (CRU, WM, GPCC, and GPCP).

semble datasets is clearly due to the simulated nature of the NCEP-2 products.

The four core precipitation datasets (CRU, WM, GPCC, GPCP) represent our current ''state-of-the-art'' understanding of global precipitation distribution. The differences among them can be viewed as estimates of the uncertainties in our collective capacity to depict spatial and temporal patterns of global rainfall. Figure 4 shows the absolute (max − min) and relative [(max − min)/(max + min)] × 100) ranges of difference between CRU, GPCC, GPCP, and Willmott–Matsuura datasets where max and min are, respectively, the highest and lowest grid cell values across the four datasets. The TRMM and NCEP-2 products were excluded because of their extreme anomalies compared to the other four data products.

The range in differences appears to be high in the wet Tropics and less so in dry regions, but the relative ranges are actually the opposite and show greater relative differences in the dry regions and more consistency in the wet regions. This finding is not surprising, but emphasizes the need to improve the sampling of precipitation in dry regions, where the relative differences between the different datasets could be as high as 100%.

c. Comparison of seasonality from the different global precipitation datasets

After analyzing the differences in mean annual total precipitation across the datasets, normalized mean monthly precipitation (P'_i) was calculated by dividing the mean monthly precipitation by the mean annual total precipitation ($P'_i = P_i/P_a$), where P_i and P_a are monthly and annual precipitation, respectively. The normalized precipitation can be viewed as the proportional distribution of the annual precipitation throughout the year. The normalization of the original datasets allowed the isolation of the seasonal differences from the inherited anomalies in the annual precipitation discussed in the previous section. The seasonal differences between the individual normalized precipitation and the normalized ensemble precipitation (P_{sd}) were calculated as $P_{sd} = [\sum_{i=1}^{12} |P'_{*i} - P'_{ei}|]/12$, where P'_{*i} is the normalized monthly precipitation according to the individual datasets and P'_{ei} is the normalized monthly ensemble precipitation.

Figure 5 shows the maxima of the seasonal differences of the four core datasets. The datasets show higher uncertainties in the seasonal partitioning of precipitation in dry regions. Apparently, the regions with high relative differences in mean annual precipitation (Fig. 4b) correspond to high uncertainties in the seasonal distribution of the precipitation. Generally, the drier regions have larger uncertainties both in terms of capturing the mean precipitation and in representing its seasonality. The only exception appears to be in the upper part of the Yukon basin where the differences in both the mean annual precipitation and seasonality are high despite the fact that this region is not extremely dry. This high uncertainty is due to the CRU dataset, which appears to have markedly different (high) precipitation values and different seasonality compared to the other three datasets (WM, GPCC, GPCP). Without having access to the raw data (the locations and the precipitation times series of the meteorological stations) used in developing

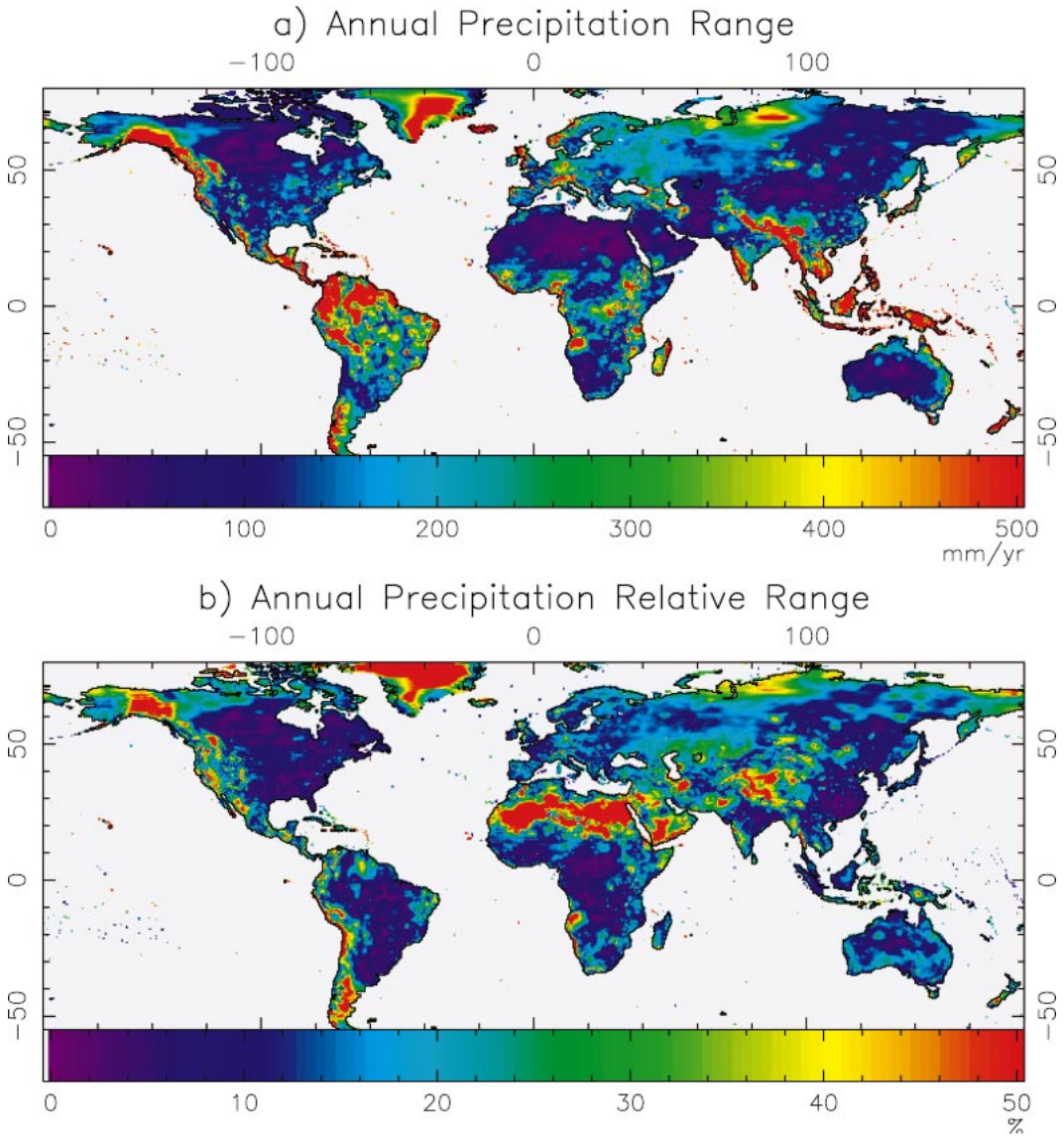

FIG. 4. Absolute and relative range of the four ''state-of-the-art'' precipitation datasets (CRU, WM, GPCC, and GPCP).

the different datasets, it is hard to identify the source of these differences and to judge which dataset provides better precipitation estimates.

4. Testing the different precipitation datasets in a water balance context

Water balance model calculations were made using long-term mean monthly input climate forcing (such as maximum, minimum, and mean air temperature, vapor pressure, cloud coverage, and wind speed) and varying individual precipitation datasets. We note again that all the climate forcings were long-term monthly averages from the CRU 95-yr time series. The precipitation was varied in order to assess the impact of the differences in the tested precipitation datasets on the resulting runoff.

Figure 6 shows the latitudinal profiles of runoff produced by the six water balance model runs. The latitudinal profiles largely have the same pattern as the precipitation profiles (Fig. 1) but the spread between the different datasets appears to be amplified.

Figures 7a and 7b show the ratios of the runoff and precipitation of absolute and relative ranges and clearly an increase in the relative range of the spatial distribution of runoffs. The apparent insensitivity of WBM in the arid regions should be noted. WBM does most poorly in extremely dry regions where rapid rain events may have the ability to produce substantial runoff despite the overall water stress. In these regions, WBM

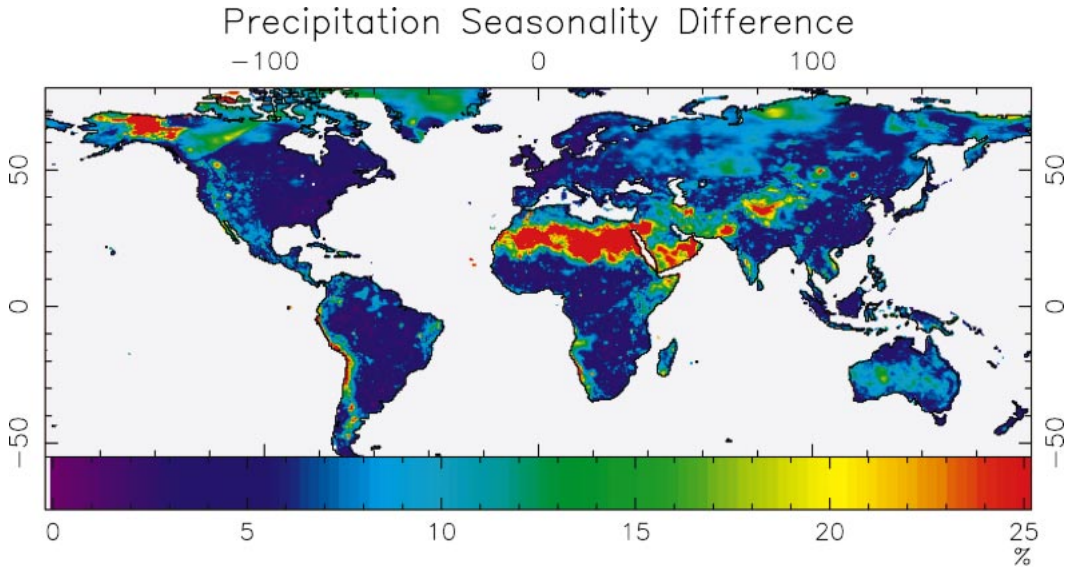

FIG. 5. Maximum seasonal differences between the four core datasets (CRU, WM, GPCC, and GPCP) and the ensemble precipitation.

tends not to produce any runoff regardless of the differences in precipitation.

The sensitivity of runoff to precipitation clearly depends on the relationship between the precipitation (P) and the potential evapotranspiration (PET). This relationship can be summarized as three classes of climate regimes:

1) Wet ($P > \text{PET}$)–the uncertainty in P translated to an uncertainty in runoff of roughly the same magnitude.
2) Semiarid ($P < \text{PET}$)–the uncertainty in P translated to less absolute uncertainty in runoff, but this runoff uncertainty in relative terms is typically higher than in the first case, due to the high nonlinearity of the evapotranspiration process.
3) Arid ($P \ll \text{PET}$)–regardless of the amount of precipitation no runoff is produced, therefore the runoff estimate is completely insensitive to the precipitation.

Figures 7a and 7b clearly show these categories. The regions showing close to 1.0 absolute runoff/precipitation range ratios are those regions in which the precipitation uncertainty translates the same uncertainty in runoff estimates. While the ratio of the absolute-ranges runoff and precipitation has an upper limit, the relative-range ratio is limitless. Figure 7b shows a high degree of runoff uncertainties in transitional zones between humid and arid regions. Regions with zero uncertainty ratios in both absolute and relative terms appear to be in the arid regions, which produce little if any runoff.

5. Summary and conclusions

Six mean monthly precipitation datasets (Climate Research Unit, Willmott–Matsuura, Global Precipitation Climate Center, Global Precipitation Climatology Project, TRMM, and NCEP–NCAR reanalysis) were compared in a water balance model context. The intercom-

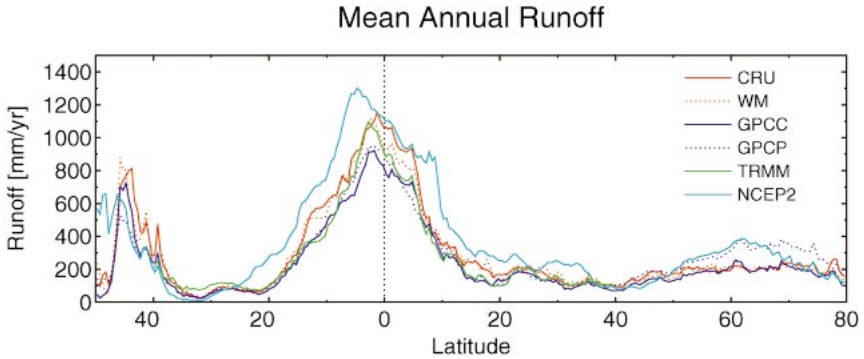

FIG. 6. Latitudinal profiles of the water balance model estimated mean annual runoff using CRU, WM, GPCC, GPCP, NCEP-2, and TRMM precipitation datasets.

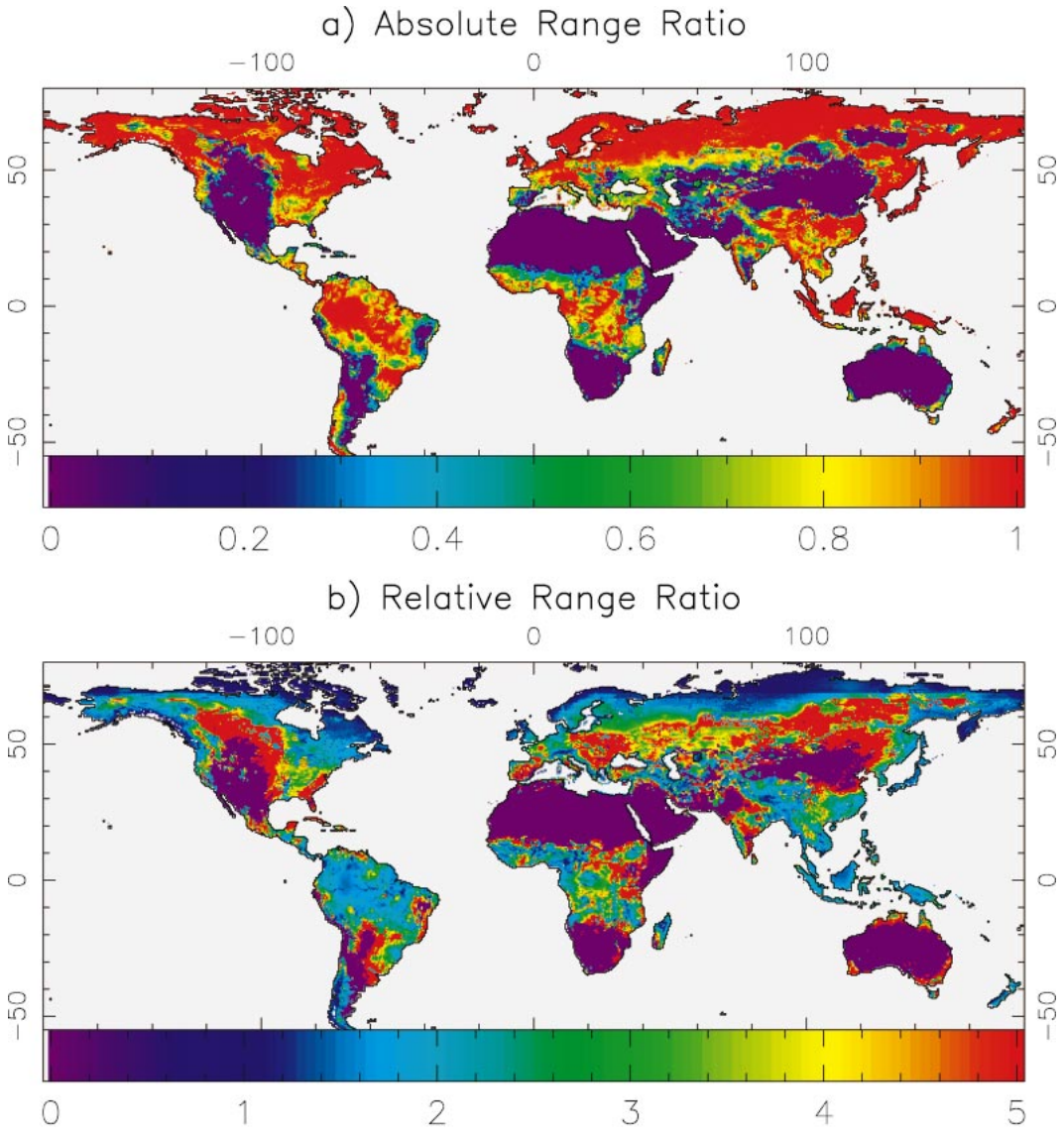

FIG. 7. Sensitivity measures arising from the use of contrasting precipitation datasets. The absolute range ratio and relative range ratio of the runoff and the precipitation were calculated by dividing the absolute and relative ranges of runoff by the absolute and relative ranges of precipitation, respectively. The figure can be viewed as the spatial distribution of the water balance calculations sensitivity to uncertainties in precipitation.

parison of individual precipitation datasets revealed substantial numerical differences, however, the overall precipitation pattern is fairly similar in each dataset. Not surprisingly, the different datasets show the largest absolute differences in the wet Tropics, but their relative performance is worse in dry regions. The range in differences between the different datasets is comparable to the total range of interannual variation of the precipitation depicted by the CRU monthly time series.

The different precipitation datasets were applied as forcings to a water balance model to estimate runoff. Comparison of the different runoff estimates showed that the uncertainty in precipitation translates to at least the same and typically much greater uncertainty in runoff in relative terms. In wet regions, where the precipitation always exceeds the potential evaporation, any error in the precipitation translates to approximately the same absolute error in runoff (which will result in higher relative error since runoff is always less than the precipitation). In semidry regions, the runoff-generation processes are highly nonlinear, therefore the errors in precipitation translate into even greater errors in the runoff. In arid regions, the water balance calculation does not produce any runoff (in some cases due to the WBM's inability to capture the impact of rapid rain events over small scales), therefore the runoff estimate is virtually insensitive to the precipitation inputs.

The present study demonstrated the significance of

potential precipitation errors in water balance calculations. Such calculations are becoming increasingly important for better water resource management as water availability is becoming recognized as one of the most important limiting natural resources for human development (Oki et al. 2001; Vörösmarty et al. 2000; Alcamo et al. 2000). The sensitivity of runoff (water supply) to precipitation uncertainties in semiarid regions demonstrates the need to make significant improvements of the precipitation monitoring in those regions as many are already under severe water stress (Vörösmarty et al. 2000; Vörösmarty et al. 2003, manuscript submitted to *Ambio*).

Comparison of simulated runoff to observed river discharge has the potential to objectively assess the performance of various precipitation datasets. Unfortunately, the availability of river discharge data is limited and in a rapid decline after the mid-1980s (Vörösmarty et al. 2002; Shiklomanov et al. 2002). Thus, the comparison of the tested datasets to corresponding discharge datasets globally was not possible for the present study and likely future studies.

Acknowledgments. This work was supported by NASA TRMM (NAJ5-4785), NASA Cooperative Agreement (NCC5-304), NASA EOS (NAG5-11750), NASA GEWEX (NAG5-10135), NASA (NAG5-11738, NAG5-11599) as well as NOAA NA17RJ1231. We also would like to thank Kenju Matsuura for his contribution in creating the Willmott–Matsuura (2001) dataset.

REFERENCES

Adler, R. F., C. Kidd, G. Petty, M. Morissey, and H. M. Goodman, 2001: Intercomparison of global precipitation products: The Third Precipitation Intercomparison Project (PIP-3). *Bull. Amer. Meteor. Soc.,* **82,** 1377–1396.

Alcamo, J., T. Henrichs, and T. Rösch, 2000: World water in 2025: Global modeling and scenario analysis. *World Water Scenarios,* F. R. Rijsberman, Ed., Earthscan, 204–271.

Costa, M. H., and J. A. Foley, 1998: A comparison of precipitation datasets for the Amazon basin. *Geophys. Res. Lett.,* **25,** 155–158.

CRU, cited 2000: Climate Research Unit, University of East Anglia. [Available online at http://www.cru.uea.ac.uk.]

FAO/UNESCO, 1986: Gridded FAO/UNESCO Soil Units. UNEP/GRID, FAO Soil Map of the World in Digital form, Digital Raster Data on 2-minute Geographic (lat × lon) 5400 × 10800 grid, UNEP/GRID, Carouge, Switzerland.

Federer, C. A., C. Vörösmarty, and B. M. Fekete, 1996: Intercomparison of methods for calculating potential evaporation in regional and global water balance models. *Water Resour. Res.,* **32,** 2315–2321.

——, ——, and ——, 2003: Sensitivity of annual evaporation to soil and root properties in two models of contrasting complexity. *J. Hydrometeor.,* **4,** 1276–1290.

Fekete, B. M., 2001: Spatial distribution of global runoff and its storage in river channels. Ph.D. thesis, University of New Hampshire, 137 pp.

GPCC, cited 2001: Global Precipitation Climate Center. [Available online at http://www.dwd.de/research/gpcc.]

GPCP, cited 1998: Global Precipitation Climatology Project. [Available online at http://orbit-net.nesdis.noaa.gov/arad/gpcp.]

Huffman, G. J., 1997: Estimates of root-mean-square random error for finite samples of estimated precipitation. *J. Appl. Meteor.,* **36,** 1191–1201.

——, R. F. Adler, B. Rudolf, U. Schneider, and P. R. Kehn, 1995: Global precipitation estimates based on technique for combining satellite-based estimates, raingauge analyses and NWP model information. *J. Climatol.,* **8,** 1284–1295.

——, and Coauthors, 1997: The Global Precipitation Climatology Project (GPCP) combined precipitation dataset. *Bull. Amer. Meteor. Soc.,* **78,** 5–20.

Hutchinson, M. F., 1995: Interpolating main rainfall using thin plate smoothing splines. *Int. J. Geogr. Info. Syst.,* **9,** 385–403.

Kalnay, E., and Coauthors, 1996: The NCEP/NCAR 40-Year Reanalysis Project. *Bull. Amer. Meteor. Soc.,* **77,** 437–472.

Kanamitsu, M., W. Ebisuzaki, J. Woolen, S.-K. Yang, J. J. Hnilo, M. Fiorino, and G. L. Potter, 2002: NCEP-DOE AMIP-II Reanalysis (R-2). *Bull. Amer. Meteor. Soc.,* **83,** 1631–1643.

Kistler, R., and Coauthors, 2001: The NCEP/NCAR 50-Year Reanalysis: Monthly means CD-ROM and documentation. *Bull. Amer. Meteor. Soc.,* **82,** 247–267.

Legates, D. R., and C. J. Willmott, 1990: Mean seasonal and spatial variability in gauge-corrected, global precipitation. *Int. J. Climatol.,* **10,** 111–127.

Melillo, J. M., A. D. McGuire, D. W. Kicklighter, B. Moore III, C. J. Vörösmarty, and A. L. Schloss, 1993: Global climate change and terrestrial net primary production. *Nature,* **363,** 234–240.

New, M., M. Hume, and P. Jones, 1999: Representing twentieth century space–time climate variability: I. Development of a 1961–1990 mean monthly terrestrial climatology. *J. Climatol.,* **12,** 829–856.

——, ——, and ——, 2000: Representing twentieth century space–time climate variability: II. Development of 1901–1996 monthly grids of terrestrial surface. *J. Climatol.,* **13,** 2217–2238.

Oki, T., T. Nishimura, and P. Dirmeyer, 1999: Assessment of annual runoff from land surface models using Total Runoff Integrating Pathways (TRIP). *J. Meteor. Soc. Japan,* **77,** 235–255.

——, Y. Agata, S. Kanae, T. Saruhashi, D. Yang, and K. Musiake, 2001: Global, assessment of current water resources using total runoff integrating pathways. *Hydrol. Sci. J.,* **46,** 983–996.

Roads, J. O., 2003: The NCEP–NCAR, NCEP–DOE, and TRMM tropical atmosphere hydrologic cycles. *J. Hydrometeor.,* **4,** 826–840.

——, S.-C. Chen, M. Kanamitsu, and H. Juang, 1999: Surface water characteristics in the NCEP Global Spectral Model and Reanalysis. *J. Geophys. Res.,* **104** (D16), 19 307–19 327.

——, M. Kanamitsu, and R. Stewart, 2002: CSE water and energy budgets in the NCEP–DOE Reanalysis II. *J. Hydrometeor.,* **3,** 227–248.

Rudolf, B., W. Rueth, and U. Schneider, 1994: Terrestrial precipitation analysis: Operational method and required density of point measurements. *Global Precipitation and Climate Change,* M. Desbois and F. Desahmond, Eds., Springler-Verlag, 173–186.

Shepard, D., 1968: A two-dimensional interpolation function for irregularly-spaced data. *Proc. 23rd ACM National Conf.,* Princeton, NJ, Association for Computing Machinery, 517–523.

Shiklomanov, A. I., R. B. Lammers, and C. J. Vörösmarty, 2002: Widespread decline in hydrological monitoring threatens pan-Arctic research. *Eos, Trans. Amer. Geophys. Union,* **83,** 16–17.

Shuttleworth, W. J., and J. S. Wallace, 1985: Evaporation from sparse crops—An energy combination theory. *Quart. J. Roy. Meteor. Soc.,* **111,** 839–855.

Susskind, J., P. Piraino, L. Rokke, L. Iredell, and A. Mehta, 1997: Characteristics of the TOVS Pathfinder Path A dataset. *Bull. Amer. Meteor. Soc.,* **78,** 1449–1472.

Thornthwaite, C. W., 1948: An approach toward a rational classification of climate. *Geogr. Rev.,* **38,** 55–94.

——, and J. R. Mather, 1955: The water balance. *Publ. Climatol.,* **8,** 1–104.

Vörösmarty, C. J., B. Moore III, A. L. Grace, M. Gildea, J. M. Melillo, B. J. Peterson, E. B. Rastetter, and P. A. Steudler, 1989: Con-

tinental scale models of water balance and fluvial transport: An application to South America. *Global Biochem. Cycles,* **3,** 241–265.
——, C. J. Willmott, B. J. Choudhury, A. L. Schloss, T. K. Streans, S. M. Robeson, and T. J. Dorman, 1996: Analyzing the discharge regime of a large tropical river through remote sensing, ground-based climatic data and modeling. *Water Resour. Res.,* **32,** 3137–3150.
——, C. A. Federer, and A. L. Schloss, 1998: Potential evaporation functions compared on U.S. watersheds: Possible implications for global-scale water balance and terrestrial ecosystem modeling. *J. Hydrol.,* **207,** 147–169.
——, P. Green, J. Salisbury, and R. B. Lammers, 2000: Global water resources: Vulnerability from climate change and population growth. *Science,* **289,** 284–288.
——, and Coauthors, 2002: Global water data: A newly endangered species. *Eos, Trans. Amer. Geophys. Union,* **82,** 54, 56, 58.
Wahba, G., 1979: How to smooth curves and surfaces with splines and cross-validation. *Proc. 24th Conf. on the Design of Experiments,* U.S. Army Research Office, Rep. 79-2, 167–192.
Willmott, C. J., and S. M. Robeson, 1995: Climatologically Aided Interpolation (CAI) of terrestrial air temperature. *Int. J. Climatol.,* **15,** 221–229.
——, and K. Matsuura, cited 2001: Terrestrial air temperature and precipitation: Monthly and annual time series (1950–1999) Version 1.02. [Available online at http://climate.geog.udel.edu/climate.]
——, C. M. Rowe, and Y. Mintz, 1985a: Climatology of the terrestrial seasonal water cycle. *J. Climatol.,* **5,** 589–606.
——, ——, and W. D. Philpot, 1985b: Small-scale climate maps: A sensitivity analysis of some common assumptions associated with grid-point interpolation and contouring. *Amer. Cartogr.,* **12,** 5–16.
——, S. M. Robeson, and M. J. Janis, 1996: Comparison of approaches for estimating time-averaged precipitation using data from the USA. *Int. J. Climatol.,* **16,** 1103–1115.